Electronic Supplementary Material (ESI) for Journal of Materials Chemistry C.

Non-fused Ring Electron Acceptors with Ethynylene Linker for Non-Halogenated Solvent-Processed Organic Solar Cell

Dou Luo,[ab] Aung Ko Ko Kyaw,*[c] Tingting Dai,[d] Erjun Zhou,[d] and Wai-Yeung Wong*[ab]

[a] *Department of Applied Biology and Chemical Technology and Research Institute for Smart Energy, The Hong Kong Polytechnic University, Hung Hom, Hong Kong, PR China*

[b] *The Hong Kong Polytechnic University Shenzhen Research Institute, Shenzhen 518057, PR China*

[c] *Guangdong University Key Laboratory for Advanced Quantum Dot Displays and Lighting, Department of Electrical & Electronic Engineering, Southern University of Science and Technology, Shenzhen 518055, China.*

[d] *National Center for Nanoscience and Technology, Beijing 100190, China*

* Corresponding author, E-mail address: aung@sustech.edu.cn (Prof. A. K. K. Kyaw); wai-yeung.wong@polyu.edu.hk (Prof. W.-Y. Wong)

1.1 General Measurement and Characterization

^{1}H NMR and ^{13}C NMR spectra were recorded on a Bruker Ascend 400 MHz spectrometer. High-resolution mass spectra were obtained with Thermo Scientific™ Q-Exactive. Elemental analyses (EAs) of compounds were performed on Vario EL cube with CHNS pattern in Fudan University (Shanghai, China).

UV-Vis-NIR absorption spectra were recorded on a Shimadzu UV-3600 UV-Vis-NIR spectrometer. The PL spectra were measured by using a HORIBA LabRAM HR Evolution spectrometer and 532 as an excitation source. The neat PAcT-Cl, CAcT-Cl and J52:PAcT-Cl, J52:CAcT-Cl films were spin-cast on quartz glass from 12 mg mL^{-1} $CHCl_3$ solution (total concentration) at a speed of 2000 rpm. Raman spectra were tested using a HORIBA LabRAM HR Evolution spectrometer and 532 nm laser as an excitation source.

Atomic force microscopy (AFM) measurements were carried out using a NanoMan VS microscope in the tapping mode. TEM images were obtained from a JEM-2100F instrument.

1.2 Organic Solar Cells Fabrication and Characterization

All devices were fabricated based on conventional structure: ITO/PEDOT:PSS/active layer/PDINN/Ag. ITO-coated glass substrates were cleaned by sonification in acetone, detergent, deionized water, and isopropyl alcohol and dried in a nitrogen stream. The pre-cleaned ITO substrates were coated with PEDOT:PSS (filtered through a 0.45 μm PES filter) by spin-coating (4000 rpm. for 30 s, thickness of ~30 nm) and then baked at 150 °C on a hotplate for 15 min in air. The PEDOT:PSS-coated ITO substrates were transferred into a N_2-filled glove box for subsequent steps. The total concentration of J52:acceptor (1:1.2 weight ratio) was fixed at 18 mg mL^{-1}, and the blend films were obtained by spin coating solutions at 1800 rpm for 45 s in *o*-xylene containing 0.5% 1-chloronaphthalene (CN) (v:v 99.5:0.5) as additive. All the optimized thickness is approximately 100 nm as measured by the profilometer. Before spin-coating, the electron transporting layer and all types of active layers were thermally annealed at 100 °C for 10 min. Finally, 5 nm of the perylene diimide functionalized (PDINN) (1 mg mL^{-1} in methanol) was spin-coated at 3000 rpm for 30 s on the active layer followed by the deposition of 100 nm Ag cathode under a under high vacuum (< 2 $\times 10^{-4}$ Pa). All the active devices area were 0.058 cm^2

through a shadow mask. The current density–voltage (*J–V*) curves were measured using Keithley 2400 source meter under 1 sun (AM 1.5 G spectrum) generated from AAA class solar simulator (Japan, SAN-EI, XES-40S1). The external quantum efficiency (EQE) spectra were measured using a Solar Cell Spectral Response Measurement System QE-R3011 (Enlitech Co., Ltd.). The light intensity at each wavelength was calibrated using a standard single crystal Si photovoltaic cell.

1.3 Fabrication of Single-Carrier Devices

Single-carrier device (ITO/PEDOT:PSS(40 nm)/active layer/MoO_3(10 nm)/Ag) and (ITO/ZnO(40 nm)/active layer/PDINN/Ag) were fabricated to measure hole and electron mobilities of the blend films. The active layers were spin-cast from *o*-xylene solution at 1800 rpm for 45 s (total concentration, 16 mg mL^{-1}). The thickness was approximately 100 nm as measured by the profilometer for all the binary and ternary films. The as-cast pure films of PAcT-Cl and CAcT-Cl were spin-cast from chloroform solution (total concentration, 10 mg mL^{-1}) at 2200-2400 rpm for 30 s. The thickness is approximately between 50-60 nm.

The mobility μ was derived from the SCLC model which is described by the equation $J = (9/8)\varepsilon_0\varepsilon_r\mu(V^2/d^3)$,[1] where J is the current, ε_0 the permittivity of free space, ε_r the relative permittivity of the material, d the thickness of the active layers, and V the effective voltage.

1.4 Photo-CELIV Test

Photo-CELIV was conducted on all-in-one platform of Paios (Fluxim AG). A light pulse with duration of 50 μs generated from a white LED lamp (light intensity 100%) was applied prior to a voltage ramp from 0.05 to 1 V μs^{-1}. The charge carrier mobility (μ) was calculated from the equation, $\mu = 2d^2/[3At_{max}^2(1+0.36\Delta j/j(0))]$, where d is the active layer thickness, A is the voltage ramp, t_{max} is the maximum current time, Δj is the peak transient current, and $j(0)$ is the displacement current.

1.5 Femtosecond (fs) Transient Absorption (TA) Spectroscopy Characterization

For femtosecond transient absorption spectroscopy, the fundamental output from Yb:KGW laser (1030 nm, 220 fs Gaussian fit, 100 kHz, Light Conversion Ltd) was split into two light beams. One was introduced to NOPA (ORPHEUS-N, Light Conversion Ltd) to produce a certain wavelength for pump beam, the other was focused onto a YAG plate to generate white light continuum as probe beam. The pump and probe overlapped on the sample at a small angle less

than 10°. The transmitted probe light from sample was collected by a linear CCD array. A pump pulse of 800 nm (below 5 μJ/cm^2) was employed to excite only acceptors and after a certain delay time, the relative transmittance change (ΔA) was probed using a white-light continuum. The primary absorption peaks for different acceptors and donors are well separated in the spectral domain, therefore, both the spectral and temporal characteristics of hole transfer dynamics can be extracted.

1.6 Contact Angle Measurements

The contact angle tests were performed on a Dataphysics OCA40 Micro surface contact angle analyzer. The surface energy of the polymers was characterized and calculated by the contact angles of the two probe liquids with the Wu model.[2,3]

$$\frac{4\gamma_{water}^{d}\gamma_{s}^{d}}{\gamma_{water}^{d}+\gamma_{s}^{d}}+\frac{4\gamma_{water}^{p}\gamma_{s}^{p}}{\gamma_{water}^{p}+\gamma_{s}^{p}}=\gamma_{water}(1+\cos\theta_{water})$$

$$\frac{4\gamma_{oil}^{d}\gamma_{s}^{d}}{\gamma_{oil}^{d}+\gamma_{s}^{d}}+\frac{4\gamma_{oil}^{p}\gamma_{s}^{p}}{\gamma_{oil}^{p}+\gamma_{s}^{p}}=\gamma_{oil}(1+\cos\theta_{oil})$$

where γ_s is the total surface energy of acceptors and polymers, and γ_s^d and γ_s^p are the dispersion and polar components of γ_s, the values of γ_{water}^{d}, γ_{water}^{p}, γ_{oil}^{d}, γ_{oil}^{p} could be found from the literature and θ is the droplet contact angle between sample and probe liquid.

1.7 Materials and Synthesis

All manipulations involving air-sensitive reagents were performed under an inert atmosphere of dry nitrogen. Compounds **1**[4], **5**[5] and **6**[6] were synthesized according to the method in the literature. All the other starting materials, unless otherwise specified, were purchased commercially and used as received without further purification.

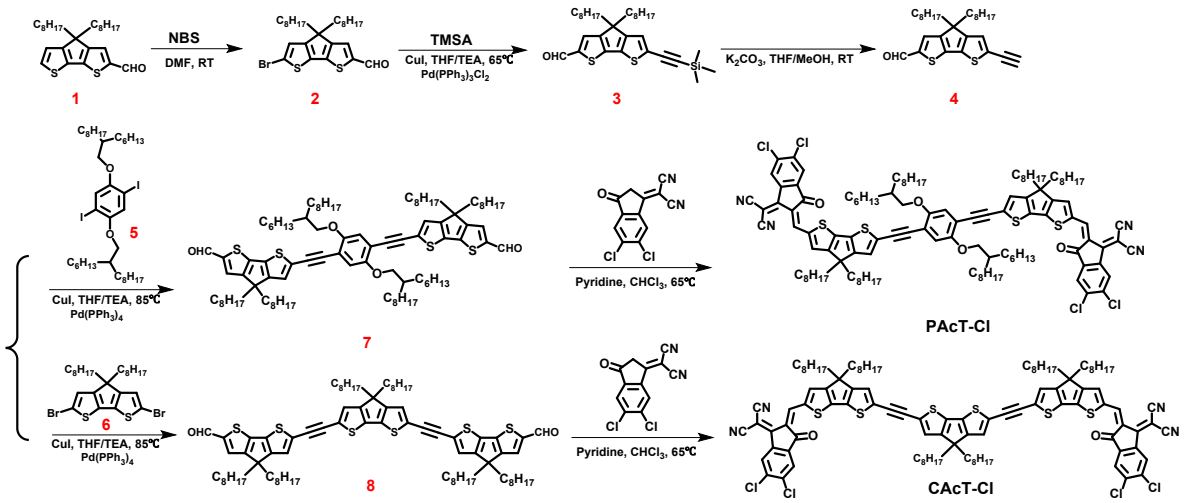

Scheme S1. Synthetic routes of PAcT-Cl and CAcT-Cl.

Synthesis of 6-bromo-4,4-dioctyl-4H-cyclopenta[2,1-b:3,4-b']dithiophene-2-carbaldehyde **(2)**

Compound **1** (2 g, 4.64 mmol) was added in 30 mL DMF under a nitrogen atmosphere. N-Bromosuccinimide (908 mg, 5.10 mmol) was then added dropwise to the solution and the mixture was stirred for another 4 h. Then the mixture was poured into water and extracted with CH_2Cl_2 for three times. The organic layer was washed with water and then dried over $MgSO_4$. After removal of solvent, the crude product was purified on a silica-gel column chromatography using petroleum ether/ dichloromethane as the eluent to afford a yellow oil (2.22 g, 94 %). ^{1}H NMR (400 MHz, $CDCl_3$, ppm): δ 9.83 (s, 1H), 7.55 (s, 1H), 7.01 (s, 1H), 1.89-1.76 (m, 4H), 1.25-0.92 (m, 24H), 0.86-0.83 (m, 6H). HRMS: calcd for $C_{26}H_{37}BrOS_2$, 509.61; found, 509.6 (100%).

Synthesis of 4,4-dioctyl-6-((trimethylsilyl)ethynyl)-4H-cyclopenta[2,1-b:3,4-b']dithiophene-2-carbaldehyde **(3)**

A mixture of compound **2** (1 g, 1.96 mmol), $Pd(PPh_3)_2Cl_2$ (41.31 mg, 0.058 mmol), CuI (11.2 mg, 0.058 mmol), 10 mL anhydrous THF and 5 mL triethylamine was deoxygenated with a nitrogen for 15 min. TMSA (481.7 mg, 4.9 mmol) was added quickly under a nitrogen atmosphere via syringe. The reaction was heated at 85 °C for 12 h. After being cooled to room temperature, the mixture was poured into water and extracted with CH_2Cl_2 for three times. The organic layer was washed with water and then dried over $MgSO_4$. After removal of solvent, the crude product was purified on a silica-gel column chromatography using petroleum ether/CH_2Cl_2 as the eluent to afford a yellow oil (875 mg, 85 %). ^{1}H NMR (400 MHz, $CDCl_3$, ppm): 9.84 (s, 1H), 7.55 (s, 1H), 7.11 (s, 1H), 1.89-1.77 (m, 4H), 1.30-0.90 (m, 24H), 0.86-0.83 (m, 6H), 0.27 (s, 9H). HRMS: [M] calcd for $C_{31}H_{46}OS_2Si$, 526.91; found, 526.81 (100%).

Synthesis of 6-ethynyl-4,4-dioctyl-4H-cyclopenta[2,1-b:3,4-b']dithiophene-2-carbaldehyde **(4)**

To a solution of **3** (500 mg) in THF (10 mL), methanol (10 mL) and K_2CO_3 (655 mg, 4.74 mmoL) were added and the mixture was stirred for 4 h. The mixture was poured into water and extracted with CH_2Cl_2 for three times. The organic layer was washed with water and then dried over $MgSO_4$. After removal of solvent, the crude product was purified on a silica-gel column chromatography using petroleum ether/CH_2Cl_2 as the eluent to afford a yellow oil (428 mg, 99 %). ^{1}H NMR (400 MHz, $CDCl_3$, ppm): 9.85 (s, 1H), 7.56 (s, 1H), 7.15 (s, 1H), 3.53 (s, 1H), 1.85-1.83 (m, 4H), 1.25-0.92 (m, 24H), 0.86-0.83 (m, 6H). HRMS: [M] calcd for $C_{28}H_{38}OS_2$, 454.73; found, 454.2 (100%).

Synthesis of 6,6'-((2,5-bis((2-hexyldecyl)oxy)-1,4-phenylene)bis(ethyne-2,1-diyl))bis(4,4-dioctyl-4H-cyclopenta[2,1-b:3,4-b']dithiophene-2-carbaldehyde) **(7)**

A mixture of compound **4** (302 mg, 0.664 mmol), compound **5** (244.7 mg, 0.302 mmol), CuI (3.45 mg, 0.018 mmol), 15 mL anhydrous THF and 5 mL triethylamine was deoxygenated with nitrogen for 15 min. $Pd(PPh_3)_4$ (21.3 mg, 0.018 mmol) was added quickly under a nitrogen atmosphere via syringe. The reaction was heated at 85 ^{o}C for 12 h. After being cooled to room temperature, the mixture was poured into water and extracted with CH_2Cl_2 for three times. The organic layer was washed with water and then dried over $MgSO_4$. After removal of solvent, the crude product was purified on a silica-gel column chromatography using petroleum ether/CH_2Cl_2 as the eluent to afford a red solid (375.9 mg, 85 %). ^{1}H NMR (400 MHz, $CDCl_3$, ppm): δ 9.82 (s, 2H), 7.57 (s, 2H), 7.14 (s, 2H), 6.98 (s, 2H), 3.97-3.81 (m, 4H), 1.90-1.82 (m, 8H), 1.47-1.27 (m, 50H), 1.21-0.96 (m, 48H), 0.90-0.85 (m, 24H). HRMS: [M] calcd for $C_{94}H_{142}O_4S_4$, 1464.41; found, 1464.50 (100%).

Synthesis of 6,6'-((4,4-dioctyl-4H-cyclopenta[2,1-b:3,4-b']dithiophene-2,6-diyl)bis(ethyne-2,1-diyl))bis(4,4-dioctyl-4H-cyclopenta[2,1-b:3,4-b']dithiophene-2-carbaldehyde) **(8)**

A mixture of compound **4** (450 mg, 0.989 mmol), compound **6** (241 mg, 0.43 mmol), CuI (4.91 mg, 0.026 mmol), 15 mL anhydrous THF and 5 mL triethylamine was deoxygenated with nitrogen for 15 min. $Pd(PPh_3)_4$ (29.82 mg, 0.025 mmol) was added quickly under a nitrogen atmosphere via syringe. The reaction was heated at 85 ^{o}C for 12 h. After being cooled to room temperature, the mixture was poured into water and extracted with CH_2Cl_2 for three times. The organic layer was washed with water and then dried over $MgSO_4$. After removal of solvent, the

crude product was purified on a silica-gel column chromatography using petroleum ether/CH_2Cl_2 as the eluent to afford a red solid (489.3 mg, 87 %). ^{1}H NMR (400 MHz, $CDCl_3$, ppm): δ 9.85 (s, 2H), 7.57 (s, 2H), 7.22 (s, 2H), 7.15 (s, 2H), 1.93-1.76 (m, 12H), 1.31-1.15 (m, 60H), 1.02-0.89 (m, 12H), 0.87-0.83 (m, 18H). HRMS: [M] calcd for $C_{81}H_{110}O_2S_6$, 1308.13; found, 1308.47 (100%).

Synthesis of 2,2'-((2Z,2'Z)-((((2,5-bis((2-hexyldecyl)oxy)-1,4-phenylene)bis(ethyne-2,1-diyl))bis(4,4-dioctyl-4H-cyclopenta[2,1-b:3,4-b']dithiophene-6,2-diyl))bis(methanylylidene)) bis(5,6-dichloro-3-oxo-2,3-dihydro-1H-indene-2,1-diylidene))dimalononitrile **(PAcT-Cl)**

2-(5,6-Dichloro-3-oxo-2,3-dihydro-1H-inden-1-ylidene)malononitrile (173 mg, 0.657 mmol) was added to a solution of compound **7** (420 mg, 0.286 mmol) in $CHCl_3$ (30 mL) under a nitrogen atmosphere. Then 1 mL pyridine was injected into the solution. The mixture was stirred at 60 °C for 12 h. After being cooled to room temperature, the mixture was poured into water and extracted with CH_2Cl_2. The organic layer was washed with water and then dried over $MgSO_4$. After removal of solvent, the crude product was purified on a silica-gel column chromatography using CH_2Cl_2 as the eluent. **PAcT-Cl** was obtained as a black solid (434 mg, 80%). ^{1}H NMR (400 MHz, $CDCl_3$, ppm): δ 8.92 (s, 2H), 8.74 (s, 2H), 7.90 (s, 2H), 7.64 (s, 2H), 7.16 (s, 2H), 6.97 (s, 2H), 3.94-3.92 (d, 4H), 1.92-1.90 (m, 10H), 1.41-1.71 (m, 80H), 0.97-0.83 (m, 32H). ^{13}C NMR (151 MHz, $CDCl_3$) δ 186.11, 165.44, 160.42, 158.36, 153.90, 139.79, 139.24, 138.98, 138.62, 137.81, 135.99, 131.82, 126.81, 126.29, 124.87, 119.48, 115.54, 114.80, 114.57, 113.63, 95.55, 89.61, 72.21, 68.02, 54.18, 38.10, 37.81, 31.95, 31.79, 31.46, 30.14, 29.92, 29.80, 29.66, 29.35, 29.27, 26.91, 24.71, 22.61, 14.10. HRMS: [M] calcd for $C_{118}H_{146}Cl_4N_4O_4S_4$ 1954.53; found, 1954.53. Anal. Calcd. for $C_{118}H_{146}Cl_4N_4O_4S_4$: C 72.51, H 7.53, N 2.87, S 6.56; found: C 72.50, H 7.62, N 2.81, S 6.60.

Synthesis of 2,2'-((2Z,2'Z)-((((4,4-dioctyl-4H-cyclopenta[2,1-b:3,4-b']dithiophene-2,6-diyl)bis(ethyne-2,1-diyl))bis(4,4-dioctyl-4H-cyclopenta[2,1-b:3,4-b']dithiophene-6,2-diyl))bis (methanylylidene))bis(5,6-dichloro-3-oxo-2,3-dihydro-1H-indene-2,1-diylidene))dimalononitrile **(CAcT-Cl)**

2-(5,6-Dichloro-3-oxo-2,3-dihydro-1H-inden-1-ylidene)malononitrile (191 mg, 0.726 mmol) was added to a solution of compound **8** (380 mg, 0.29 mmol) in $CHCl_3$ (30 mL) under a nitrogen atmosphere. Then 1 mL pyridine was injected into the solution. The mixture was stirred at 60 °C

for 12 h. After being cooled to room temperature, the mixture was poured into water and extracted with CH_2Cl_2. The organic layer was washed with water and then dried over $MgSO_4$. After removal of solvent, the crude product was purified on a silica-gel column chromatography using CH_2Cl_2 as the eluent. **CAcT-Cl** was obtained as a black solid (427.6 mg, 82%). ^{1}H NMR (400 MHz, $CDCl_3$, ppm): δ 8.91-8.89 (d, 2H), 8.72 (s, 2H), 7.90-7.88 (d, 2H), 7.64-7.62 (d, 2H), 7.26-7.16 (m, 4H), 1.92-1.84 (m, 12H), 1.26-1.18 (m, 60H), 0.97-0.83 (m, 30H). ^{13}C NMR (151 MHz, $CDCl_3$) δ 186.13, 165.46, 164.45, 160.44, 159.48, 158.29, 140.23, 139.79, 139.41, 139.25, 139.00, 138.61, 137.70, 135.95, 131.19, 128.93, 127.09, 126.80, 126.12, 124.89, 122.93, 119.42, 114.75, 93.32, 89.47, 67.98, 54.17, 37.78, 31.78, 29.89, 29.39, 29.33, 29.25, 24.69, 22.61, 14.03. HRMS: [M] calcd for $C_{105}H_{114}Cl_4N_4O_2S_6$ 1798.25; found, 1798.39. Anal. Calcd. for $C_{105}H_{114}Cl_4N_4O_2S_6$: C 70.13, H 6.39, N 3.12, S 10.70; found: C 70.14, H 6.42, N 3.15, S 10.60.

1.8 Supporting Figures and Tables

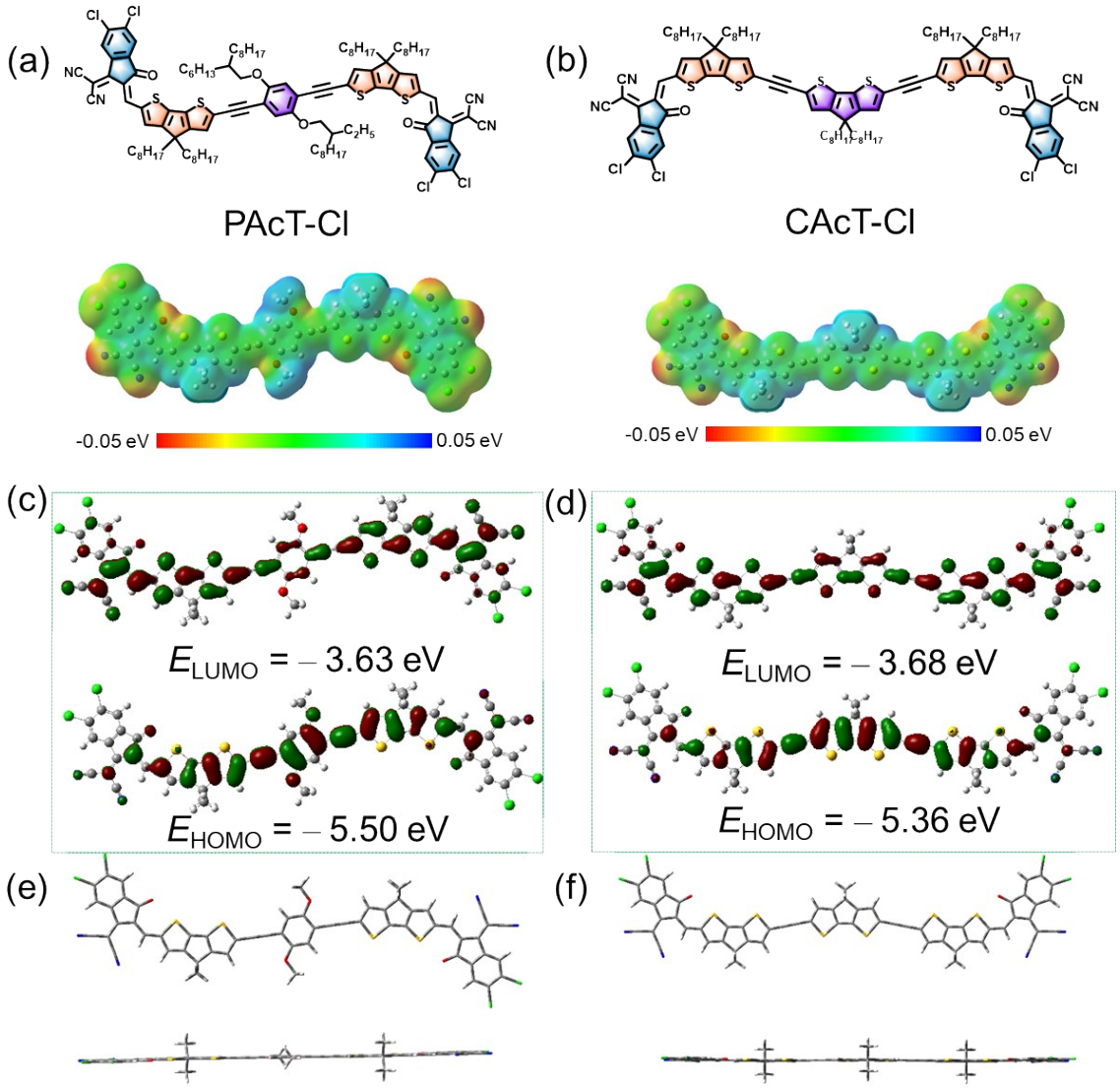

Fig. S1 Electrostatic potential (ESP) of (a) PAcT-Cl and (b) CAcT-Cl. The calculated energy levels of (c) PAcT-Cl and (d) CAcT-Cl. Calculated geometries of (e) PAcT-Cl and (f) CAcT-Cl.

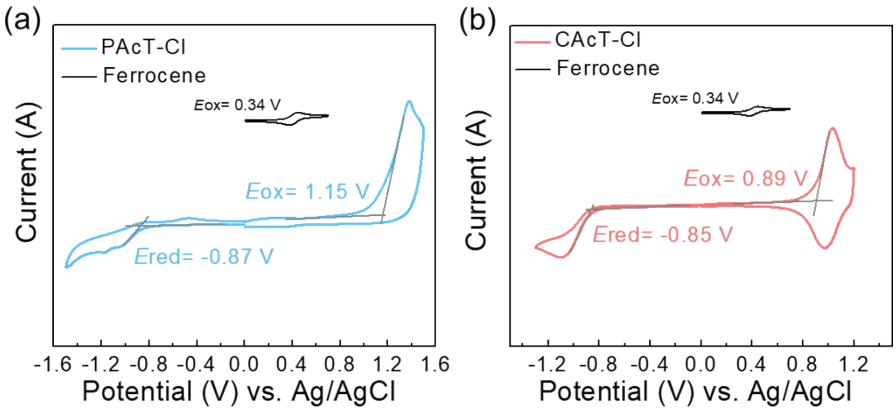

Fig. S2 CV curves of (a) PAcT-Cl and (b) CAcT-Cl.

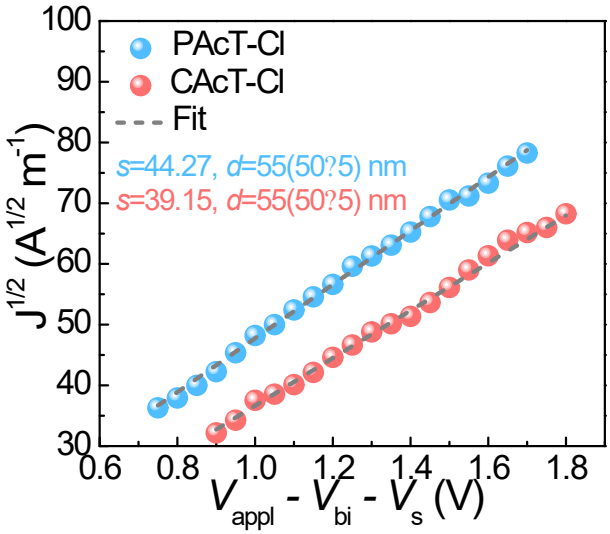

Fig. S3 The $J^{1/2}$–V characteristic of the electron-only device based on the pure films of PAcT-Cl and CAcT-Cl.

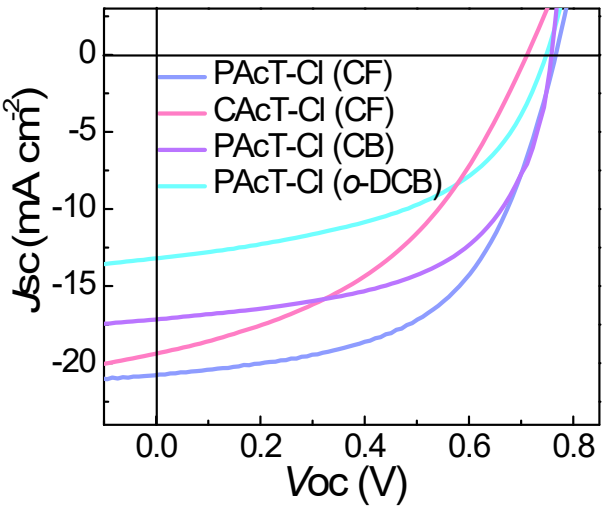

Fig. S4 J–V characteristics of the OSCs based on J52:PAcT-Cl and J52:CAcT-Cl processed with different solvents under AM1.5G illumination (100 mW cm^{-2}).

Table S1 Photovoltaic parameters of OSCs based on J52:PAcT-Cl and J52:CAcT-Cl blended films processed with different solvents.

Active layer	V_{oc} (V)	J_{sc} (mA cm^{-2})	***FF***(%)	PCE (%)[d)]
J52:PAcT-Cl (CF)[a)]	0.768	20.75	54.3	8.65
J52:CAcT-Cl (CF)[a)]	0.710	19.45	42.1	5.81
J52:PAcT-Cl (CB)[b)]	0.762	17.20	57.6	7.54
J52:PAcT-Cl (*o*-DCB)[c)]	0.750	13.13	50.7	5.00

[a)] Total concentration was 16 mg mL^{-1}, and spin coating speed was 3000 rpm for 30 s; [b)] Total concentration was 20 mg mL^{-1}, and spin coating speed was 2000 rpm for 45 s; [c)] Total concentration was 20 mg mL^{-1}, and spin coating speed was 2000 rpm for 45 s. All the solutions contained 0.5% 1-chloronaphthalene (CN) (v:v 99.5:0.5) as additive; [d)] The best-performing devices from eight devices.

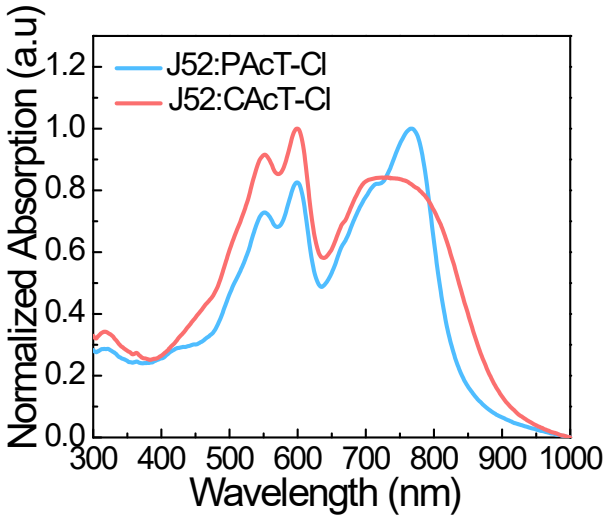

Fig. S5 UV–vis absorption spectra of J52:PAcT-Cl and J52:CAcT-Cl.

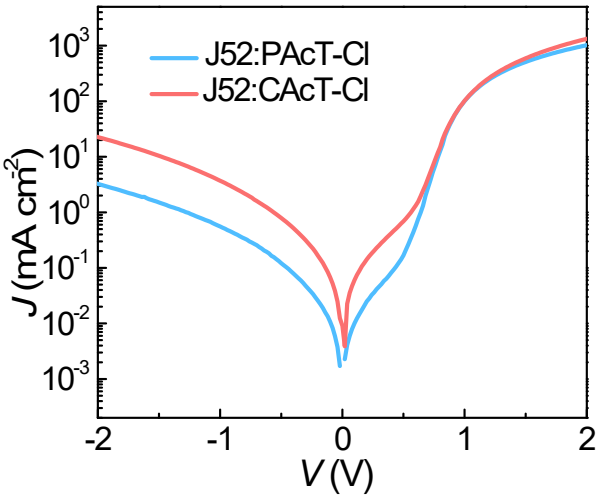

Fig. S6 Dark *J*–*V* characteristics of the photovoltaic devices based on *o*-xylene-processed J52:PAcT-Cl and J52:CAcT-Cl.

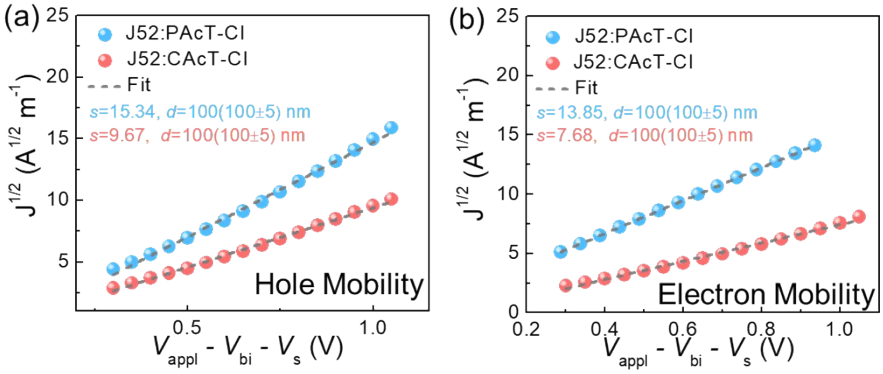

Fig. S7 The $J^{1/2}$–V characteristic of the (a) hole and (b) electron-only device based on the blend films of PAcT-Cl and CAcT-Cl.

Table S2 Hole and electron mobilities in single-carrier devices.

Blend films	μ_h ($cm^2\ V^{-1}\ s^{-1}$)	μ_e ($cm^2\ V^{-1}\ s^{-1}$)	μ_h / μ_e ratio
J52:PAcT-Cl	7.84×10^{-5}	6.39×10^{-5}	1.22
J52:CAcT-Cl	3.11×10^{-5}	1.96×10^{-5}	1.58

Table S3 Detailed parameters of TA spectra, the electron transfer kinetics (excited at 500 nm and prob at 630 nm) were fitted by a biexponential function: $i = A_1 \exp(-t/\tau_1) + A_2 \exp(-t/\tau_2)$, with two lifetimes of τ_1 and τ_2 and prefactors of A_1 and A_2.

Blend film	A_1	τ_1 (ps)	A_2	τ_2 (ps)	τ_m (ps)[a)]
J52:PAcT-Cl	0.45	1.63	0.55	99.0	97.76
J52:CAcT-Cl	0.53	2.38	0.47	128.0	125.35

[a)] The average lifetime values were extracted by a biexponential function fit and calculated according to the equation: $\tau_m = \Sigma i\ Ai\tau i / \Sigma i\ Ai$.

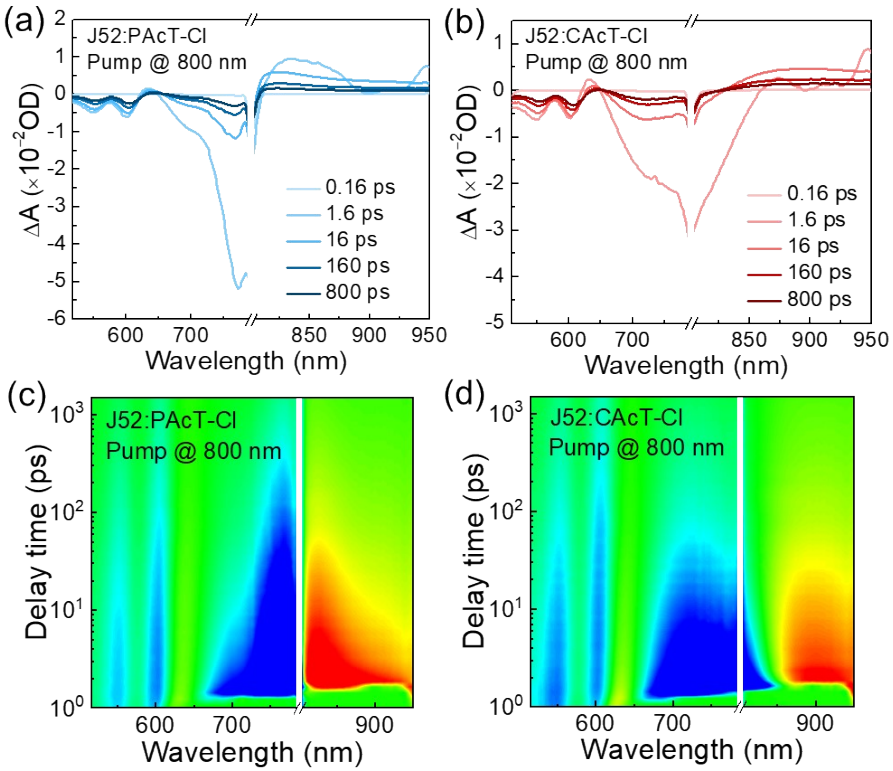

Fig. S8 Representative TA spectra of (a) J52:PAcT-Cl and (b) J52:CAcT-Cl blend films under 800 nm excitation. Color plot of TA spectra of (c) J52:PAcT-Cl and (d) J52:CAcT-Cl blend films under 800 nm excitation.

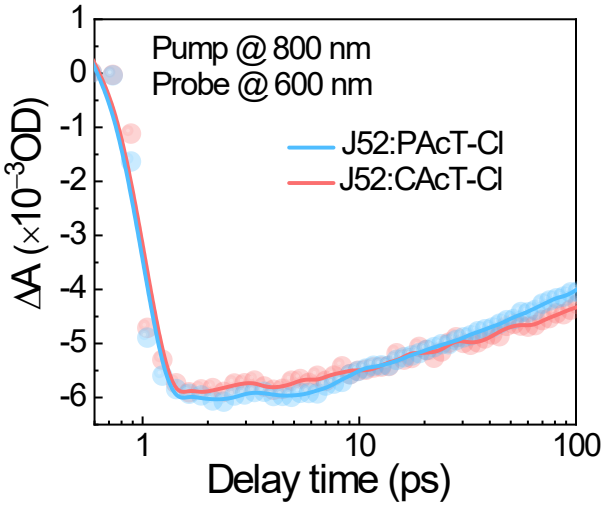

Fig. S9 The decay traces of GSB at 600 nm for the blend films with an excitation wavelength of 800 nm.

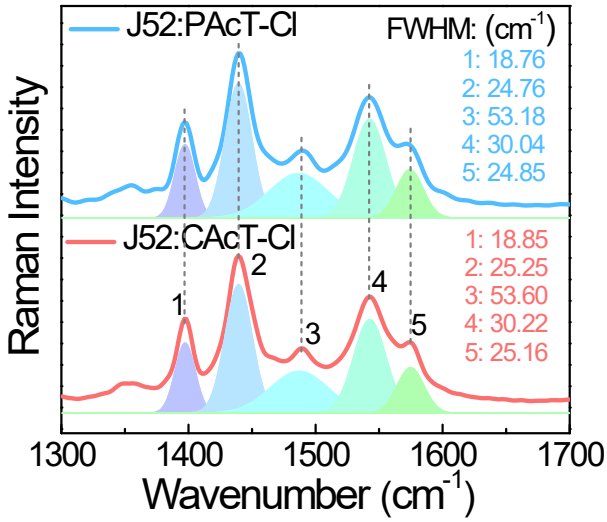

Fig. S10 Raman spectra of J52:PAcT-Cl and J52:CAcT-Cl under laser excitation at 532 nm.

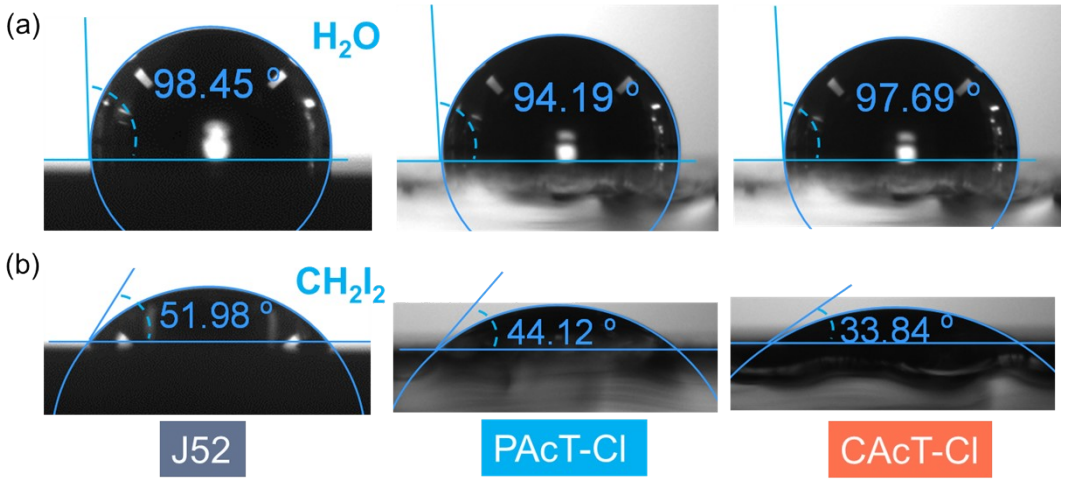

Fig. S11 Contact angles of water and diiodomethane droplets on the J52, PAcT-Cl and CAcT-Cl films.

Table S4 The contact angles and surface tension parameters of the donor and acceptors.

Pristine film	θ_{water} (deg)	θ_{DIM} (deg)	γ^d (mN/m)	γ^p (mN/m)	Surface tension (mN/m)	χ
J52	98.4	51.9	32.01	2.68	34.70	–
PAcT-Cl	94.19	44.12	35.21	3.64	38.86	0.117 *K*
CAcT-Cl	97.69	33.84	41.37	1.53	42.90	0.434 *K*

γ^d and γ^p represent the surface free energy (γ) generated from the dispersion forces and the polar forces, respectively. Surface energy (γ) = $\gamma^d + \gamma^p$

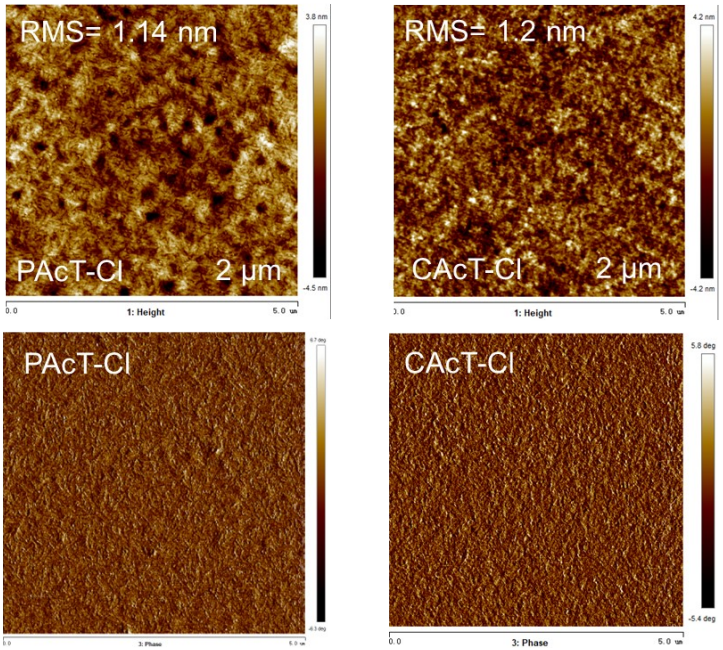

Fig. S12 Tapping-mode AFM height image of pure PAcT-Cl and CAcT-Cl films.

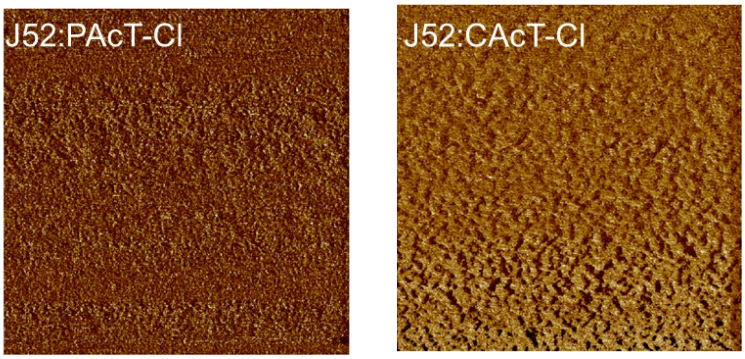

Fig. S13 The phase images of AFM for J52:PAcT-Cl and J52:CAcT-Cl blend films.

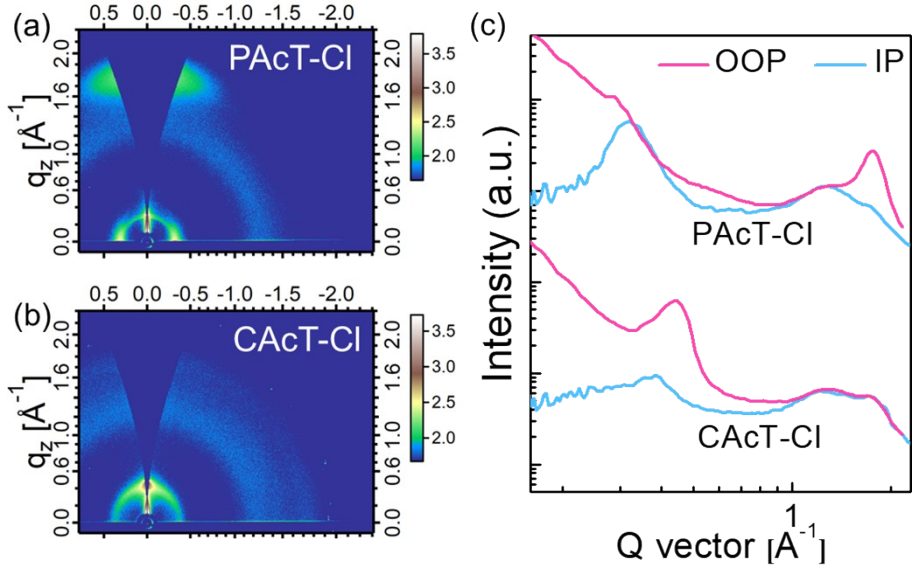

Fig. S14 GIWAXS patterns of pure (a) PAcT-Cl and (b) CAcT-Cl films. (c) Out-of-plane and in-plane line-cut profiles of the pure films.

Table S5 Morphology data of PAcT-Cl, CAcT-Cl and binary blend films.

Film	in plane (IP)				out of plane (OOP)			
	Position ($Å^{-1}$)	D-spacing[a] Å	FWHM Å	CCL[b] Å	Position ($Å^{-1}$)	D-spacing[a] Å	FWHM Å	CCL[b] Å
PAcT-Cl	0.320	19.62	0.082	68.85	1.75	3.58	0.245	23.04
CAcT-Cl	1.726	3.63	0.393	14.36	0.438	14.33	0.124	45.53
J52:PAcT-Cl	0.309	20.32	0.064	88.21	1.77	3.54	0.374	15.09
J52:CAcT-Cl	0.319	19.68	0.113	49.96	1.76	3.56	0.376	15.01

[a] Obtained using the equation of $d = 2\pi/q$, in which q is the corresponding x-coordinate of the diffraction peak. [b] Calculated using the equation: $CCL = 2\pi K/w$, in which w is the full width at half maxima and K is a form factor.

1.9 ^{1}H NMR, ^{13}C NMR and HRMS Spectra of PAcT-Cl and CAcT-Cl

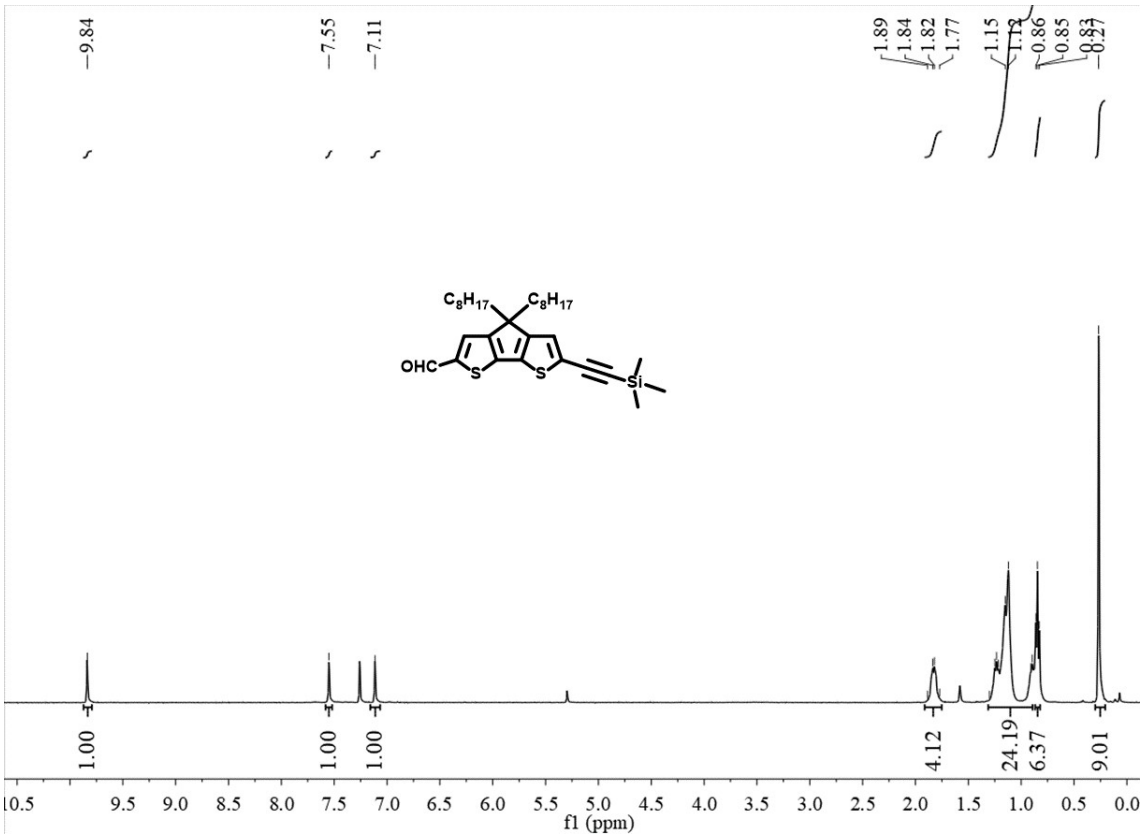

Fig. S15. ^{1}H NMR spectrum of compound **3** ($CDCl_3$, 400 MHz).

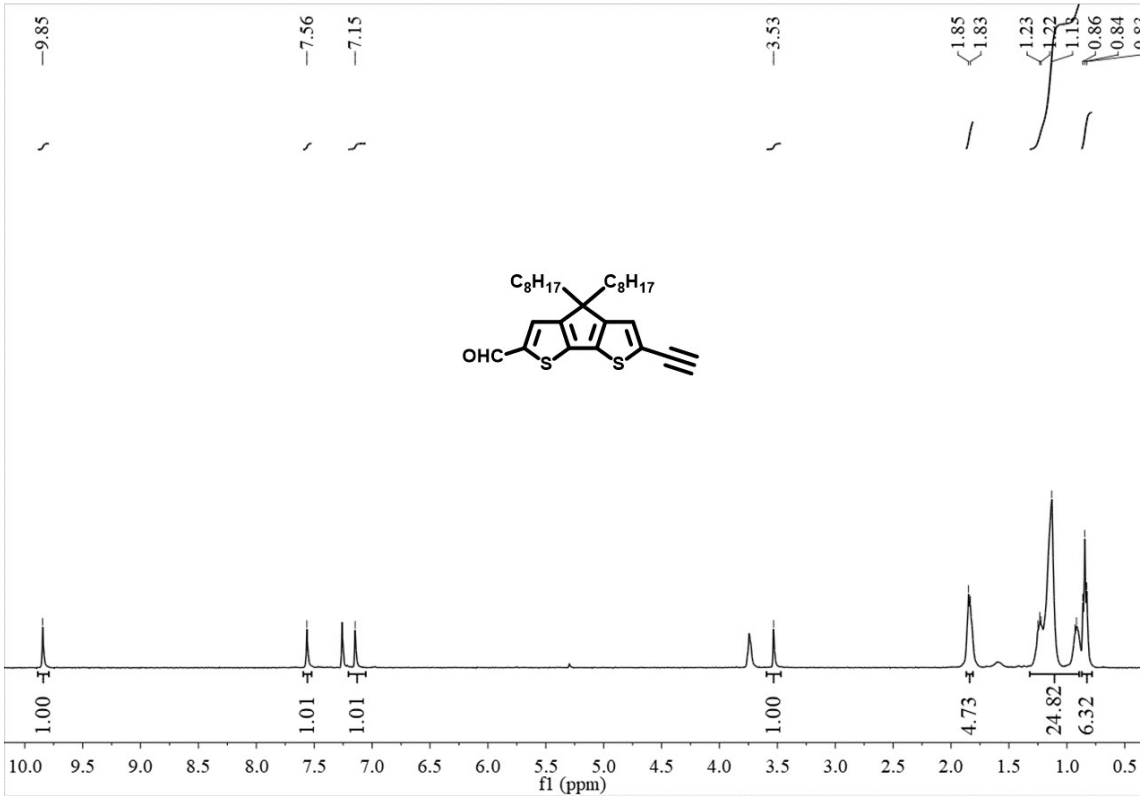

Fig. S16. ^{1}H NMR spectrum of compound **4** ($CDCl_3$, 400 MHz).

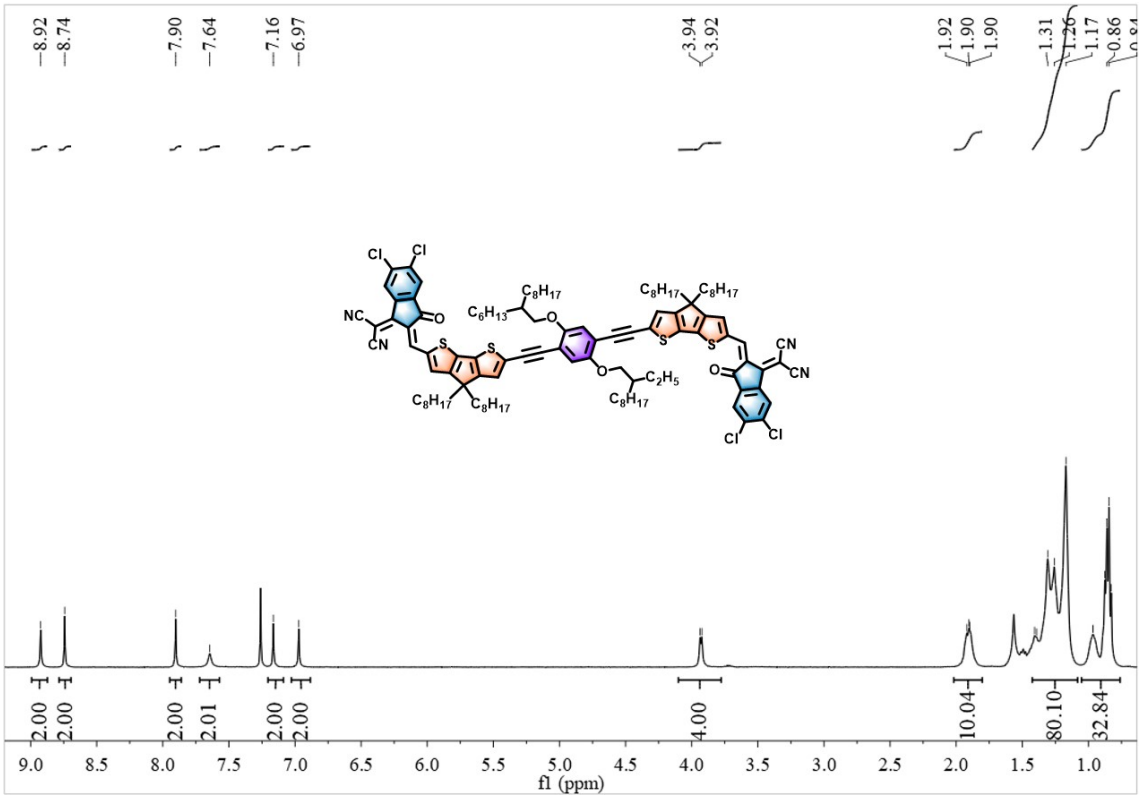

Fig. S17. ^{1}H NMR spectrum of PAcT-Cl ($CDCl_3$, 400 MHz).

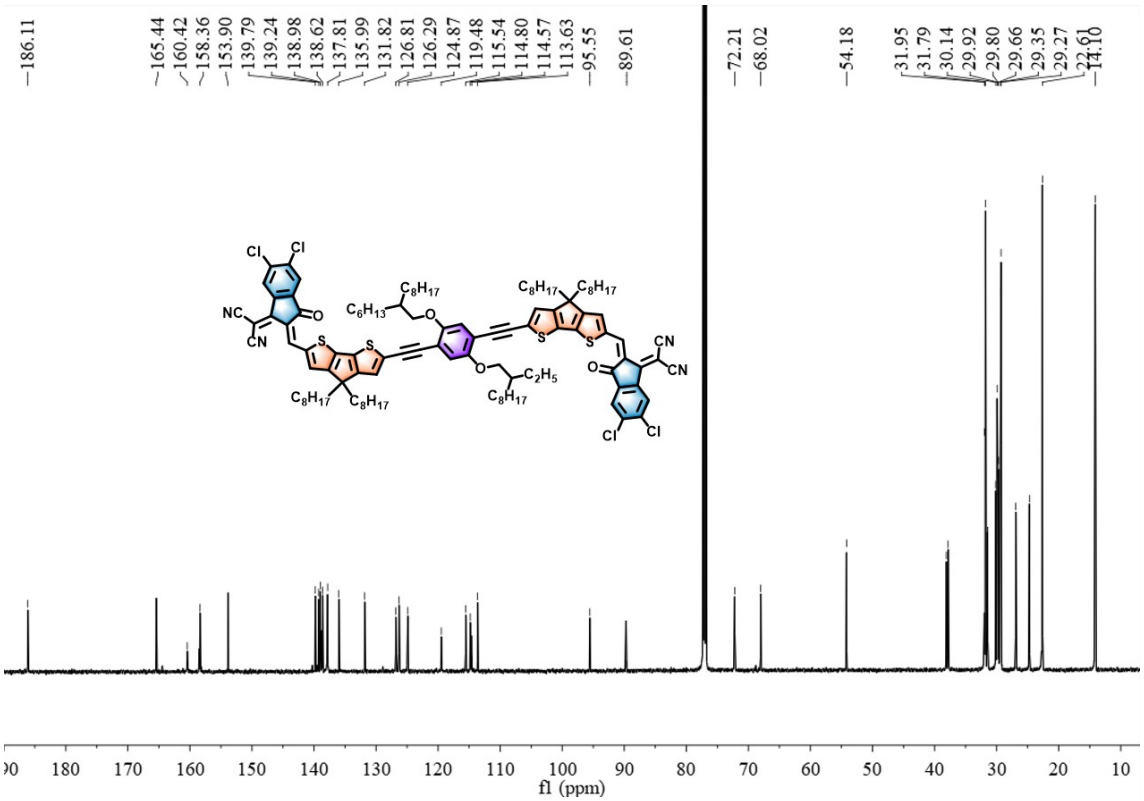

Fig. S18. ^{13}C NMR spectrum of compound PAcT-Cl ($CDCl_3$, 400 MHz).

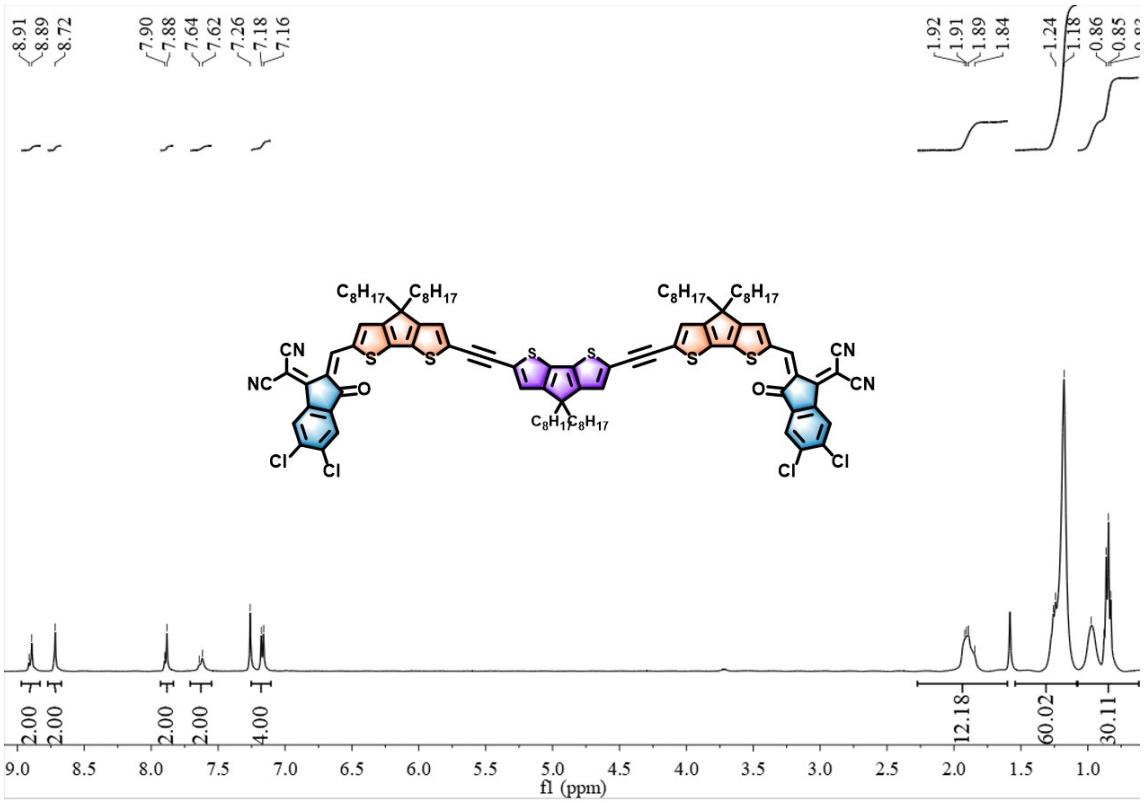

Fig. S19. ^{13}H NMR spectrum of compound CAcT-Cl ($CDCl_3$, 400 MHz).

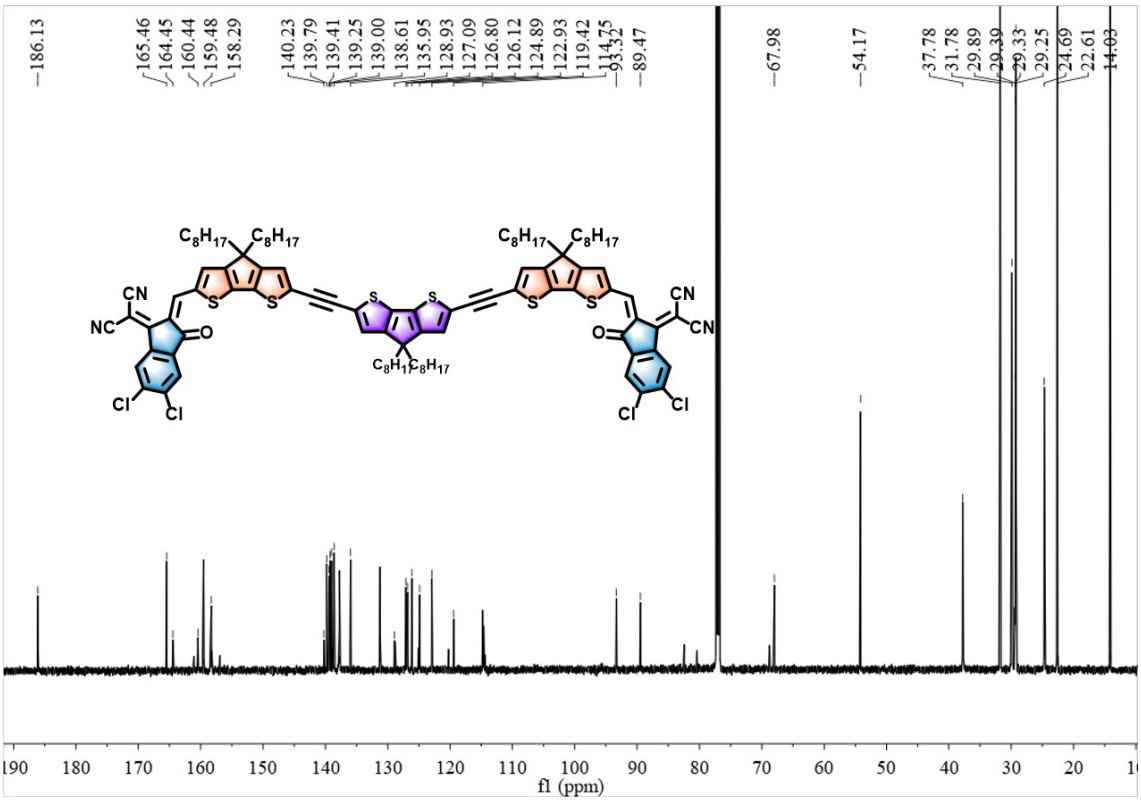

Fig. S20. ^{13}C NMR spectrum of compound CAcT-Cl ($CDCl_3$, 400 MHz).

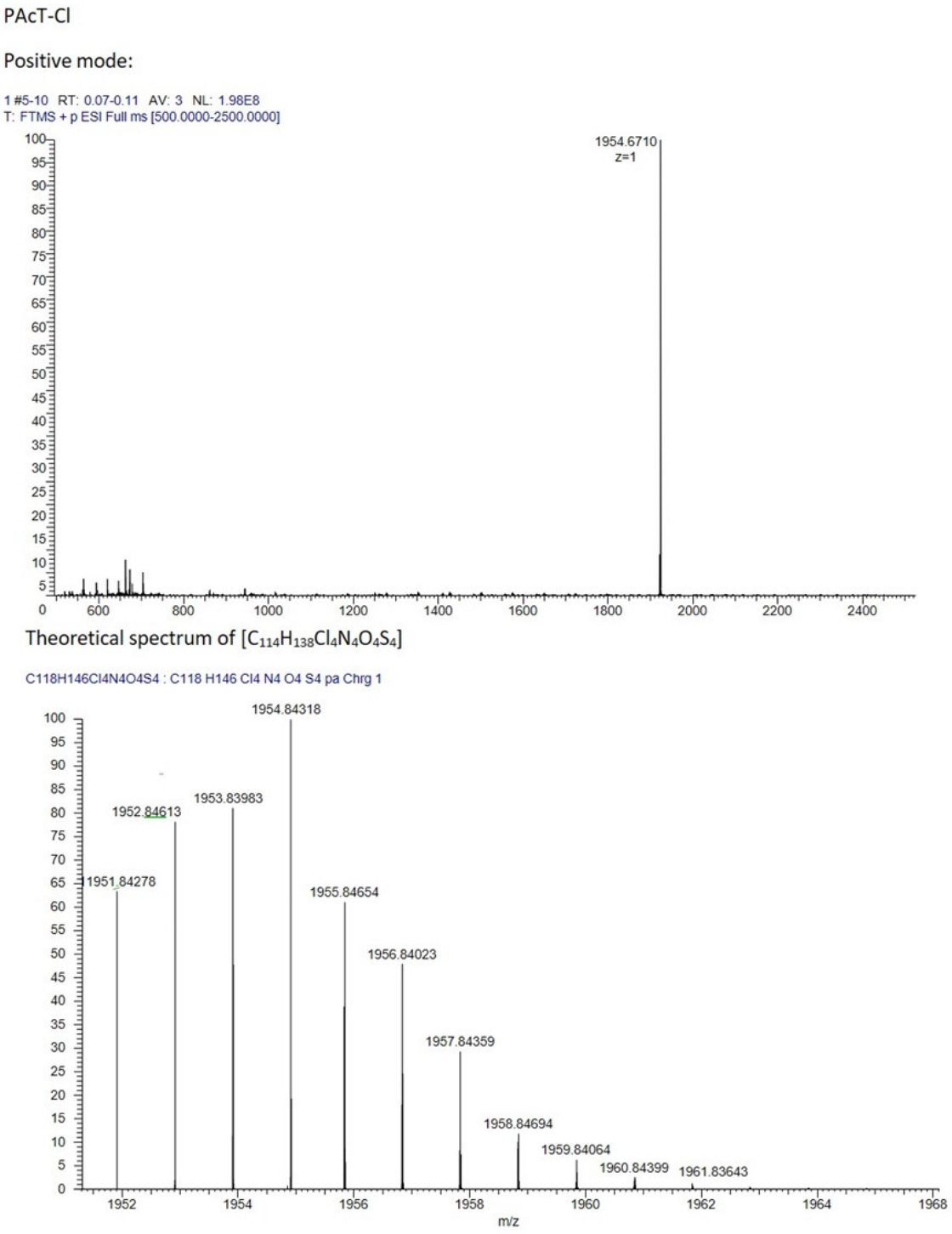

Fig. S21. HRMS of PAcT-Cl.

CAcT-Cl

Positive mode:

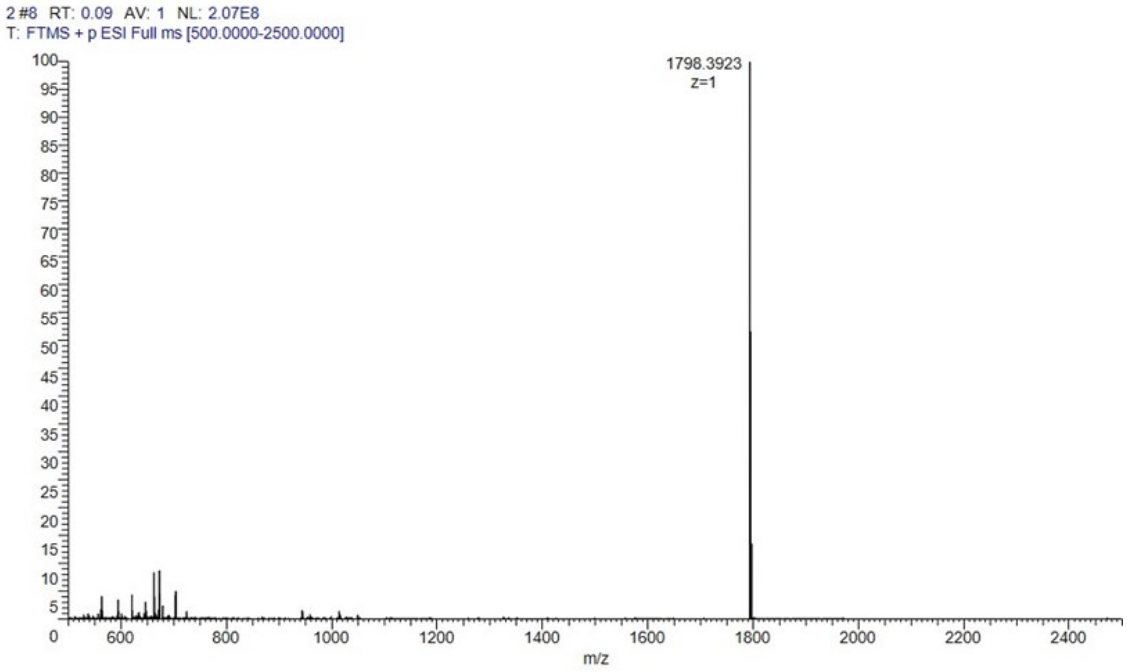

Zoom in, $[C_{105}H_{114}Cl_4N_4O_2S_6+H]^+$

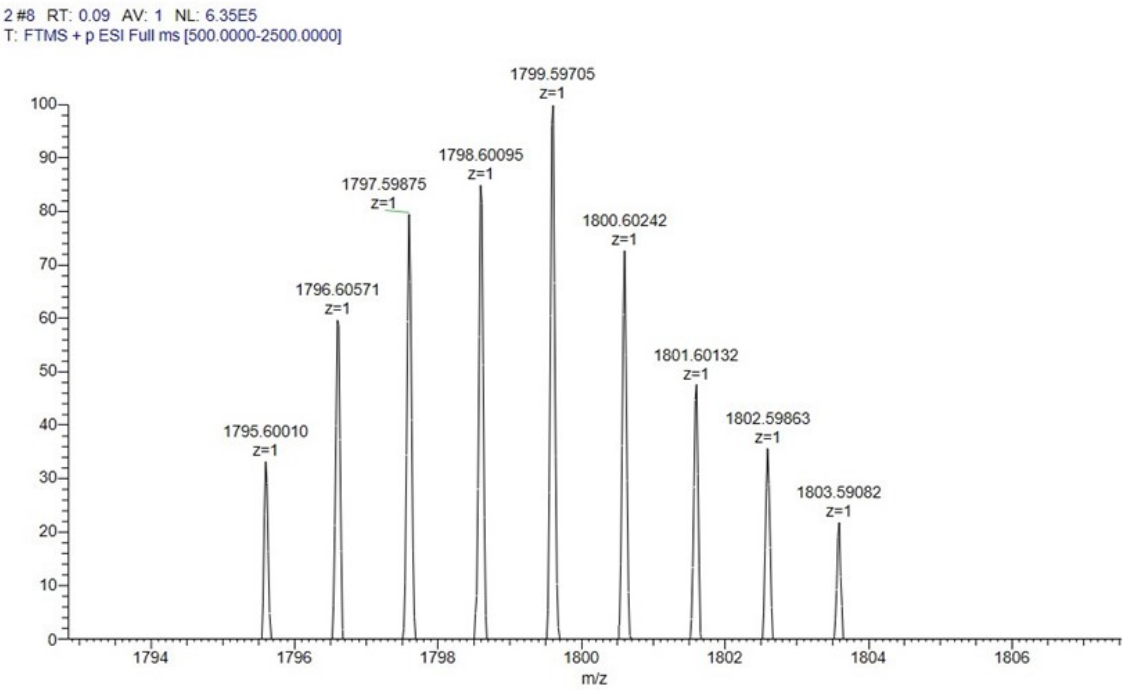

Fig. S22. HRMS of CAcT-Cl.

References

[1] Y. Sun, J. H. Seo, C. J. Takacs, J. Seifter and A. J. Heeger, *Adv*. *Mater*., 2011, **23**, 1679-1683.

[2] S. Wu, *J Adhes*. 1973, **5**, 39-55.

[3] J. Comyn, *Int J Adhesion Adhes*. 1992, **12**, 145-149.

[4] D. Luo, X. Lai, N. Zheng, C. Duan, Z. Wang, K. Wang and A. K. K. Kyaw, *Chem. Eng. J.*, 2021, **420**, 129768.

[5] H. Usta, D. Alimli, R. Ozdemir, E. Tekin, F. Alkan, R. Kacar, A. Altas, S. Dabak, A. Gürek, E. Mutlugun, A. Yazicia and A. Cana, *J. Mater. Chem. C*, 2020, **8**, 8047-8060.

[6] S.-Y Liou, C.-S. Ke, J.-H. Chen, Y.-W. Luo, S.-Y. Kuo, Y.-H. Chen, C.-C. Fang, C.-Y. Wu, C.-M. Chiang, and Y.-H. Chan, *ACS Macro Lett.*, 2016, **5**, 154–157.